Journal of Sound and Vibration (2001) **244**(4), 651–668
doi:10.1006/jsvi.2000.3517, available online at http://www.idealibrary.com on IDEAL®

POWER FLOW MODELS AND ANALYSIS OF IN-PLANE WAVES IN FINITE COUPLED THIN PLATES

D.-H. Park and S.-Y. Hong

Department of Naval Architecture and Ocean Engineering, Seoul National University, Seoul 151-742, *Korea. E-mail: syhong@gong.snu.ac.kr*

H.-G. Kil

Department of Mechanical Engineering, The University of Suwon, Suwon 445-743, *Korea*

AND

J.-J. Jeon

Agency for Defense Development, Chinhae 645-600, *Korea*

(*Received* 24 *November* 1999, *and in final form* 23 *October* 2000)

Energy equations analogous to the thermal conductivity equation are derived to examine the propagation of longitudinal waves and in-plane shear waves in finite thin plates. The derived energy equations are expressed with the time- and locally space-averaged energy density, and can be used as the prime equations for the prediction of in-plane structural vibration energy and intensity at middle–high-frequency ranges. To the cases of finite coupled structures connected at a certain angle, the derived in-plane wave energy equation and developed flexural wave energy equation have been applied by changing the frequency and the damping loss factor to evaluate the proposed methods for the predictions of middle–high-frequency vibration energy and intensity distributions.

1. INTRODUCTION

Until recently, many of the plate vibration researches have been mainly executed for transverse vibration problems with diverse approaches, while the in-plane vibration effects and the related phenomena have not been deeply studied. For instance, in the power flow analysis (PFA) method, the energy governing equations of thin plates and membranes were derived for the propagation of flexural waves [1, 2] and thus, a single plate can be analyzed with the PFA method when transverse exciting forces are applied. However, for coupled plate structures which are joined at a certain angle and on which transverse exciting forces are applied, in-plane waves come out with the flexural waves since the incident flexural waves are partially converted to the in-plane waves at the joint part. Moreover, in high frequency ranges, the in-plane wave components can be important in the transmission of vibrational energy through the built-up structures. Therefore, to obtain reliable results, the in-plane wave components should be taken into account with the appropriate high-frequency analysis methods [3, 4].

In this paper, to analyze the vibrating structures of in-plane motions using the PFA method, the energy governing equations for the propagation of longitudinal and in-plane shear waves in thin plates are derived. Firstly, the differential equations governing the

0022-460X/01/290651 + 18 $35.00/0

in-plane motions of thin plates are separated into two uncoupled equations of longitudinal and in-plane shear wave components by using the displacement potential functions. The displacement solutions to each wave equation are substituted into the expressions for the time-averaged in-plane energy density and intensity. Then, the energy density and intensity expressions are simplified by space-averaging over a half wavelength of each in-plane wave component and can be rearranged into compact forms by neglecting all of the second and higher order terms of the structural damping loss factor with the assumption that the damping loss factors of the plates are sufficiently small. Through these steps, the general relations of in-plane wave energy and intensity are obtained, and the energy governing equations for longitudinal and in-plane shear waves are derived respectively. The developed equations are used to predict the vibrational energy and intensity distribution of thin plate structures coupled at a certain angle and excited by the transverse harmonic forces of middle–high-frequencies.

2. EQUATIONS OF LONGITUDINAL AND IN-PLANE SHEAR WAVES IN THIN PLATES

The equations governing the free in-plane vibration of an isotropic thin plate with uniform thickness have the following partial differential equation forms [5, 6]:

$$\frac{\partial^2 u}{\partial x^2} + \frac{(1-v)}{2}\frac{\partial^2 u}{\partial y^2} + \frac{(1+v)}{2}\frac{\partial^2 v}{\partial x\,\partial y} = \frac{(1-v^2)\rho}{E_c}\frac{\partial^2 u}{\partial t^2}, \tag{1}$$

$$\frac{\partial^2 v}{\partial x^2} + \frac{(1-v)}{2}\frac{\partial^2 v}{\partial y^2} + \frac{(1+v)}{2}\frac{\partial^2 u}{\partial x\,\partial y} = \frac{(1-v^2)\rho}{E_c}\frac{\partial^2 v}{\partial t^2}. \tag{2}$$

Here, u and v are x and y components of in-plane displacement in the middle plane of the plate, and ρ, E_c and v indicate the mass density, complex Young's modulus and the Poisson ratio of the plate respectively. Using the displacement vector $\mathbf{d} = u\mathbf{i} + v\mathbf{j}$, equations (1) and (2) are simply rewritten as [7]

$$\frac{(1-v)}{2}\nabla^2\mathbf{d} + \frac{(1+v)}{2}\nabla\nabla\cdot\mathbf{d} = \frac{(1-v^2)\rho}{E_c}\frac{\partial^2\mathbf{d}}{\partial t^2}. \tag{3}$$

Since the two displacement components u and v are coupled with each other as seen in equation (3), it is quite difficult to obtain the general displacement solution of this equation. Using potential functions, Lamé represented the displacement vector $\mathbf{d}$ in the form of

$$\mathbf{d}(x, y, t) = \nabla\varphi(x, y, t) + \nabla\times\boldsymbol{\Psi}(x, y, t), \tag{4}$$

where $\varphi(x, y, t)$ is a scalar quantity representing the displacement potential which corresponds to the dilational motion of plate particles, and $\boldsymbol{\Psi}(x, y, t)$ is the displacement potential which corresponds to the rotational motion and is a vector quantity normal to the plate. Substitution of equation (4) into equation (3) gives the following equation:

$$\frac{(1-v)}{2}\nabla^2(\nabla\varphi + \nabla\times\boldsymbol{\Psi}) + \frac{(1+v)}{2}\nabla\nabla\cdot(\nabla\varphi + \nabla\times\boldsymbol{\Psi})$$

$$= \frac{(1-v^2)\rho}{E_c}\frac{\partial^2}{\partial t^2}(\nabla\varphi + \nabla\times\boldsymbol{\Psi}). \tag{5}$$

Since $\nabla \cdot \nabla\varphi = \nabla^2\varphi$ and $\nabla \cdot \nabla \times \boldsymbol{\Psi} = \mathbf{0}$, equation (5) can be rewritten as

$$\nabla\left(\nabla^2\varphi - \frac{(1-\nu^2)\rho}{E_c}\frac{\partial^2\varphi}{\partial t^2}\right) + \nabla\times\left(\frac{(1-\nu)}{2}\nabla^2\boldsymbol{\Psi} - \frac{(1-\nu^2)\rho}{E_c}\frac{\partial^2\boldsymbol{\Psi}}{\partial t^2}\right) = 0. \tag{6}$$

Clearly, the displacement representation of equation (4) satisfies the equations of motion if

$$\nabla^2\varphi(x, y, t) = \frac{1}{c_l^2}\frac{\partial^2\varphi(x, y, t)}{\partial t^2} \tag{7}$$

and

$$\nabla^2\boldsymbol{\Psi}(x, y, t) = \frac{1}{c_s^2}\frac{\partial^2\boldsymbol{\Psi}(x, y, t)}{\partial t^2}. \tag{8}$$

Equations (7) and (8) are longitudinal and in-plane shear wave equations respectively. c_l and c_s are the phase velocities of longitudinal and in-plane shear waves, expressed as follows:

$$c_l = \sqrt{\frac{K_c}{\rho h}}, \quad c_s = \sqrt{\frac{G_c}{\rho}}. \tag{9}$$

$K_c = E_c h/(1-\nu^2)$ is the complex extensional stiffness. G_c is the complex shear modulus of the plate and h is the thickness of the plate.

To represent the vibrational displacements as expressed in equation (4), the following equation must be satisfied:

$$\nabla \cdot \boldsymbol{\Psi}(x, y, t) = 0 \tag{10}$$

and since the vector potential $\boldsymbol{\Psi}(x, y, z)(= \boldsymbol{\Psi}(x, y, t)\mathbf{k})$ is normal to the plate and is a function of position (x, y) and time t, the following relations can be obtained:

$$\nabla \cdot \boldsymbol{\Psi}(x, y, t) = \partial\Psi(x, y, t)/\partial z = 0. \tag{11}$$

From the longitudinal wave equation, equation (7), $\varphi(x, y, t)$ can be expressed as follows:

$$\varphi(x, y, t) = [A_l e^{j(-k_{lx}x - k_{ly}y)} + B_l e^{j(k_{lx}x - k_{ly}y)} + C_l e^{j(-k_{lx}x + k_{ly}y)} + D_l e^{j(k_{lx}x + k_{ly}y)}] \times e^{j\omega t}. \tag{12}$$

Here, k_{lx} and k_{ly} indicate the x and y components of the complex longitudinal wave number k_l, respectively, and ω is the circular frequency. From equations (4) and (12), the longitudinal wave components u_l and v_l of the in-plane displacements u and v are written as

$$u_l(x, y, t) = \cos\theta_l[Ae^{j(-k_{lx}x - k_{ly}y)} - Be^{j(k_{lx}x - k_{ly}y)} + Ce^{j(-k_{lx}x + k_{ly}y)} - De^{j(k_{lx}x + k_{ly}y)}] \times e^{j\omega t}, \tag{13}$$

$$v_l(x, y, t) = \sin\theta_l[Ae^{j(-k_{lx}x - k_{ly}y)} + Be^{j(k_{lx}x - k_{ly}y)} - Ce^{j(-k_{lx}x + k_{ly}y)} - De^{j(k_{lx}x + k_{ly}y)}] \times e^{j\omega t}, \tag{14}$$

where $A \equiv -jk_lA_l$, $B \equiv -jk_lB_l$, $C \equiv -jk_lC_l$, $D \equiv -jk_lD_l$, $\cos\theta_l \equiv k_{lx}/k_l$, and $\sin\theta_l \equiv k_{ly}/k_l$.

From the in-plane shear wave equation (8), $\Psi(x, y, t)$ can be expressed as follows:

$$\Psi(x, y, t) = [A_s e^{j(-k_{sx}x - k_{sy}y)} + B_s e^{j(k_{sx}x - k_{sy}y)} + C_s e^{j(-k_{sx}x + k_{sy}y)} + D_s e^{j(k_{sx}x + k_{sy}y)}] \times e^{j\omega t}. \quad (15)$$

Here, k_{sx} and k_{sy} indicate the x and y components of the complex in-plane shear wave number k_s respectively. From equations (4) and (15), the in-plane shear wave components u_s and v_s of the in-plane displacements u and v are written as

$$u_s(x, y, t) = \sin\theta_s[-Ae^{j(-k_{sx}x - k_{sy}y)} - Be^{j(k_{sx}x - k_{sy}y)} + Ce^{j(-k_{sx}x + k_{sy}y)} + De^{j(k_{sx}x + k_{sy}y)}] \times e^{j\omega t}, \quad (16)$$

$$v_s(x, y, t) = \cos\theta_s[Ae^{j(-k_{sx}x - k_{sy}y)} - Be^{j(k_{sx}x - k_{sy}y)} + Ce^{j(-k_{sx}x + k_{sy}y)} - De^{j(k_{sx}x + k_{sy}y)}] \times e^{j\omega t}, \quad (17)$$

where $A \equiv -jk_sA_s$, $B \equiv -jk_sB_s$, $C \equiv -jk_sC_s$, $D \equiv -jk_sD_s$, $\cos\theta_s \equiv k_{sx}/k_s$, and $\sin\theta_s \equiv k_{sy}/k_s$.

3. IN-PLANE VIBRATIONAL ENERGY AND INTENSITY OF THIN PLATES

The x component $\langle q_x \rangle$ and y component $\langle q_y \rangle$ of the time-averaged in-plane vibration intensity in the thin plates are written as

$$\langle q_x \rangle = -\frac{1}{2}\mathrm{Re}\left[G_c h\left(\frac{\partial u}{\partial y} + \frac{\partial v}{\partial x}\right)\frac{\partial v^*}{\partial t} + K_c\left(\frac{\partial u}{\partial x} + \nu\frac{\partial v}{\partial y}\right)\frac{\partial u^*}{\partial t}\right], \quad (18)$$

$$\langle q_y \rangle = -\frac{1}{2}\mathrm{Re}\left[G_c h\left(\frac{\partial u}{\partial y} + \frac{\partial v}{\partial x}\right)\frac{\partial u^*}{\partial t} + K_c\left(\frac{\partial v}{\partial y} + \nu\frac{\partial u}{\partial x}\right)\frac{\partial v^*}{\partial t}\right] \quad (19)$$

and the time-averaged total energy density of in-plane vibration of thin plates is written as

$$\langle e \rangle = \frac{1}{4}\mathrm{Re}\left[G_c h\left(\frac{\partial u}{\partial y} + \frac{\partial v}{\partial x}\right)\left(\frac{\partial u^*}{\partial y} + \frac{\partial v^*}{\partial x}\right) + K_c\left(\frac{\partial u}{\partial x} + \nu\frac{\partial v}{\partial y}\right)\frac{\partial u^*}{\partial x}\right.$$
$$\left. + K_c\left(\frac{\partial v}{\partial y} + \nu\frac{\partial u}{\partial x}\right)\frac{\partial v^*}{\partial y} + \rho h\left(\frac{\partial u}{\partial t}\frac{\partial u^*}{\partial t} + \frac{\partial v}{\partial t}\frac{\partial v^*}{\partial t}\right)\right], \quad (20)$$

where the asterisk notation indicates a complex conjugate.

4. POWER FLOW MODEL OF LONGITUDINAL WAVES IN THIN PLATES

Energy governing equations are generally expressed with group velocity [8, 9], and the in-plane vibration of thin plates has two different wave modes known as longitudinal and in-plane shear waves which have different group velocities. For this reason, the energy governing equation of in-plane vibration cannot be expressed with a single differential equation as seen in the thermal conductivity equation, but with two independent energy equations for each wave component.

Firstly, the energy governing equation for the propagation of longitudinal waves in thin plates is derived. Substituting equations (13) and (14) into equations (18)–(20), the

time-averaged intensity and total energy density of the longitudinal waves are obtained as

$$\begin{aligned}\langle q_{lx}\rangle = &-\tfrac{1}{2}\mathrm{Re}[(1-v)K_c k_l \omega \cos\theta_l \sin^2\theta_l \{-|A^{--}|^2 + |B^{+-}|^2 - |C^{-+}|^2 + |D^{++}|^2 \\ &- A^{--}(B^{+-})^* + (A^{--})^* B^{+-} - B^{+-}(C^{-+})^* + (B^{+-})^* C^{-+} \\ &- C^{-+}(D^{++})^* + (C^{-+})^* D^{++} + A^{--}(D^{++})^* - (A^{--})^* D^{++} \\ &+ A^{--}(C^{-+})^* + (A^{--})^* C^{-+} - B^{+-}(D^{++})^* - (B^{+-})^* D^{++}\} \\ &- K_c k_l \omega \cos\theta_l (\cos^2\theta_l + v\sin^2\theta_l)\{|A^{--}|^2 - |B^{+-}|^2 + |C^{-+}|^2 - |D^{++}|^2 \\ &- A^{--}(B^{+-})^* + (A^{--})^* B^{+-} + B^{+-}(C^{-+})^* - (B^{+-})^* C^{-+} \\ &- C^{-+}(D^{++})^* + (C^{-+})^* D^{++} - A^{--}(D^{++})^* + (A^{--})^* D^{++} \\ &+ A^{--}(C^{-+})^* + (A^{--})^* C^{-+} - B^{+-}(D^{++})^* - (B^{+-})^* D^{++}\}], \end{aligned} \tag{21}$$

$$\begin{aligned}\langle q_{ly}\rangle = &-\tfrac{1}{2}\mathrm{Re}[(1-v)K_c k_l \omega \sin\theta_l \cos^2\theta_l \{-|A^{--}|^2 - |B^{+-}|^2 + |C^{-+}|^2 + |D^{++}|^2 \\ &+ A^{--}(B^{+-})^* + (A^{--})^* B^{+-} + B^{+-}(C^{-+})^* - (B^{+-})^* C^{-+} \\ &- C^{-+}(D^{++})^* - (C^{-+})^* D^{++} + A^{--}(D^{++})^* - (A^{--})^* D^{++} \\ &- A^{--}(C^{-+})^* + (A^{--})^* C^{-+} - B^{+-}(D^{++})^* + (B^{+-})^* D^{++}\} \\ &- K_c k_l \omega \sin\theta_l (\sin^2\theta_l + v\cos^2\theta_l)\{|A^{--}|^2 + |B^{+-}|^2 - |C^{-+}|^2 - |D^{++}|^2 \\ &+ A^{--}(B^{+-})^* + (A^{--})^* B^{+-} - B^{+-}(C^{-+})^* + (B^{+-})^* C^{-+} \\ &- C^{-+}(D^{++})^* - (C^{-+})^* D^{++} - A^{--}(D^{++})^* + (A^{--})^* D^{++} \\ &- A^{--}(C^{-+})^* + (A^{--})^* C^{-+} - B^{+-}(D^{++})^* + (B^{+-})^* D^{++}\}], \end{aligned} \tag{22}$$

$$\begin{aligned}\langle e_l\rangle = &\tfrac{1}{4}\mathrm{Re}[2(1-v)K_c |k_l|^2 \sin^2\theta_l \cos^2\theta_l \{|A^{--}|^2 + |B^{+-}|^2 + |C^{-+}|^2 + |D^{++}|^2 \\ &- A^{--}(B^{+-})^* - (A^{--})^* B^{+-} + B^{+-}(C^{-+})^* + (B^{+-})^* C^{-+} \\ &- C^{-+}(D^{++})^* - (C^{-+})^* D^{++} + A^{--}(D^{++})^* + (A^{--})^* D^{++} \\ &- A^{--}(C^{-+})^* - (A^{--})^* C^{-+} - B^{+-}(D^{++})^* - (B^{+-})^* D^{++}\} \\ &+ K_c |k_l|^2 (\cos^4\theta_l + 2v\cos^2\theta_l \sin^2\theta_l + \sin^4\theta_l)\{|A^{--}|^2 + |B^{+-}|^2 + |C^{-+}|^2 \\ &+ |D^{++}|^2 + A^{--}(B^{+-})^* + (A^{--})^* B^{+-} + B^{+-}(C^{-+})^* + (B^{+-})^* C^{-+} \\ &+ C^{-+}(D^{++})^* + (C^{-+})^* D^{++} + A^{--}(D^{++})^* + (A^{--})^* D^{++} \\ &+ A^{--}(C^{-+})^* + (A^{--})^* C^{-+} + B^{+-}(D^{++})^* + (B^{+-})^* D^{++}\} \end{aligned}$$

$$+ Kk_{l1}^2\{|A^{--}|^2 + |B^{+-}|^2 + |C^{-+}|^2 + |D^{++}|^2$$

$$- A^{--}(B^{+-})^* - (A^{--})^*B^{+-} - B^{+-}(C^{-+})^* - (B^{+-})^*C^{-+}$$

$$- C^{-+}(D^{++})^* - (C^{-+})^*D^{++} - A^{--}(D^{++})^* - (A^{--})^*D^{++}$$

$$+ A^{--}(C^{-+})^* + (A^{--})^*C^{-+} + B^{+-}(D^{++})^* + (B^{+-})^*D^{++}\}], \tag{23}$$

where $[\,]^{\pm\pm}$ means $[\,]\times\exp(\pm \mathrm{j}k_{lx}x \pm \mathrm{j}k_{ly}y)$, and k_{lx} and k_{ly} are the x and y components of the complex longitudinal wave number k_l respectively. For small damping, complex wave numbers k_l, k_{lx} and k_{ly} are well approximated as

$$k_l = k_{l1}\left(1 - \mathrm{j}\frac{\eta_l}{2}\right), \quad k_{lx} = k_{lx1}\left(1 - \mathrm{j}\frac{\eta_l}{2}\right), \quad k_{ly} = k_{ly1}\left(1 - \mathrm{j}\frac{\eta_l}{2}\right), \tag{24}$$

where k_{l1}, k_{lx1} and k_{ly1} are the real parts of k_l, k_{lx} and k_{ly} respectively. In equation (21), the square terms, $|A^{--}|^2, \ldots, |D^{++}|^2$ are exponentially decayed in space due to structural damping, and the other terms, $A^{--}(B^{+-})^*, \ldots, (B^{+-})^*D^{++}$ are spatially harmonic. Here, no obvious relations between intensity (equations (21) and (22)) and energy density (equation (23)) are found.

Assuming that the structural damping for the longitudinal motion of the plate is sufficiently small, all of the second and higher order terms of the structural damping loss factor are neglected. Then, the intensity and energy density are space-averaged over a half wavelength of the longitudinal wave as follows [2]:

$$\langle \overline{e_l} \rangle = \frac{k_{lx1}k_{ly1}}{\pi^2}\int_0^{\pi/k_{ly1}}\int_0^{\pi/k_{lx1}} \langle e_l \rangle \,\mathrm{d}x\,\mathrm{d}y, \tag{25}$$

$$\langle \overline{\mathbf{q}_l} \rangle = \frac{k_{lx1}k_{ly1}}{\pi^2}\int_0^{\pi/k_{ly1}}\int_0^{\pi/k_{lx1}} \langle \mathbf{q}_l \rangle \,\mathrm{d}x\,\mathrm{d}y. \tag{26}$$

The space- and time-averaged intensity and energy density are obtained as

$$\langle \overline{q_{lx}} \rangle = \tfrac{1}{2}Kk_{lx1}\omega(|A|^2e^{--} - |B|^2e^{+-} + |C|^2e^{-+} - |D|^2e^{++}), \tag{27}$$

$$\langle \overline{q_{ly}} \rangle = \tfrac{1}{2}Kk_{ly1}\omega(|A|^2e^{--} + |B|^2e^{+-} - |C|^2e^{-+} - |D|^2e^{++}) \tag{28}$$

and

$$\langle \overline{e_l} \rangle = \tfrac{1}{2}Kk_{l1}^2(|A|^2e^{--} + |B|^2e^{+-} + |C|^2e^{-+} + |D|^2e^{++}), \tag{29}$$

where for simplicity, $e^{\pm\pm} \equiv \exp(\pm\eta_l k_{lx1}x \pm \eta_l k_{ly1}y)$ and these expressions are related in the following manner:

$$\langle \overline{\mathbf{q}_l} \rangle = -\frac{c_{gl}^2}{n_l\omega}\left(\frac{\partial}{\partial x}\mathbf{i} + \frac{\partial}{\partial y}\mathbf{j}\right)\langle \overline{e_l} \rangle. \tag{30}$$

Equation (30) is the expression for the energy transmission of longitudinal waves in thin plates with damping and is analogous to Fourier's law of heat transfer.

If no input powers flow into the medium, the steady state energy balance equation of an elastic medium has the form [2]

$$-\nabla\cdot\mathbf{q}+\pi_{diss}=0, \tag{31}$$

where π_{diss} is the dissipated power due to the structural damping of the plate. Since it is known that the time-averaged dissipation power at a point in an elastic medium vibrating at circular frequency ω is proportional to the time-averaged total energy density, $\langle e\rangle$, we can write that [10]

$$\langle\pi_{diss}\rangle=\eta\omega\langle e\rangle. \tag{32}$$

The combination of equations (30)–(32) yields an energy governing equation for the space- and time-averaged longitudinal wave energy density in plates with the form

$$-\frac{c_{gl}^2}{\eta_l\omega}\left(\frac{\partial^2}{\partial x^2}+\frac{\partial^2}{\partial y^2}\right)\langle\overline{e_l}\rangle+\eta\omega\langle\overline{e_l}\rangle=0, \tag{33}$$

where c_{gl} is the group velocity of the longitudinal waves in a plate expressed as follows and is equal to the phase velocity:

$$c_{gl}=\sqrt{\frac{K}{\rho h}}. \tag{34}$$

Here, we have obtained the energy governing equation, equation (33), for the longitudinal plane waves in a thin plate, and the primary variable is the total longitudinal wave energy density space-averaged over a half wavelength and time-averaged over one period.

5. POWER FLOW MODEL OF IN-PLANE SHEAR WAVES IN THIN PLATES

In this section, the energy governing equation for the propagation of in-plane shear waves in thin plates is derived. Substituting equations (16) and (17) into equations (18)–(20), the time-averaged intensity and total energy density of in-plane shear waves are obtained as

$$\begin{aligned}\langle q_{sx}\rangle=&-\tfrac{1}{2}\mathrm{Re}[G_c h k_s\omega\cos\theta_s(\sin^2\theta_s-\cos^2\theta_s)\{|A^{--}|^2-|B^{+-}|^2+|C^{-+}|^2-|D^{++}|^2\\&-A^{--}(B^{+-})^*+(A^{--})^*B^{+-}+B^{+-}(C^{-+})^*-(B^{+-})^*C^{-+}\\&-C^{-+}(D^{++})^*+(C^{-+})^*D^{++}-A^{--}(D^{++})^*+(A^{--})^*D^{++}\\&+A^{--}(C^{-+})^*+(A^{--})^*C^{-+}-B^{+-}(D^{++})^*-(B^{+-})^*D^{++}\}\\&+(1-\nu)K_c k_s\omega\cos\theta_s\sin^2\theta_s\{-|A^{--}|^2+|B^{+-}|^2-|C^{-+}|^2+|D^{++}|^2\\&-A^{--}(B^{+-})^*+(A^{--})^*B^{+-}-B^{+-}(C^{-+})^*+(B^{+-})^*C^{-+}\\&-C^{-+}(D^{++})^*+(C^{-+})^*D^{++}+A^{--}(D^{++})^*-(A^{--})^*D^{++}\\&+A^{--}(C^{-+})^*+(A^{--})^*C^{-+}-B^{+-}(D^{++})^*-(B^{+-})^*D^{++}\}],\end{aligned} \tag{35}$$

$$\begin{aligned}\langle q_{sy}\rangle = &-\tfrac{1}{2}\,\mathrm{Re}[G_c h k_s \omega \sin\theta_s(\sin^2\theta_s - \cos^2\theta_s)\{-|A^{--}|^2 - |B^{+-}|^2 + |C^{-+}|^2 + |D^{++}|^2 \\ &- A^{--}(B^{+-})^* - (A^{--})^* B^{+-} + B^{+-}(C^{-+})^* - (B^{+-})^* C^{-+} \\ &+ C^{-+}(D^{++})^* + (C^{-+})^* D^{++} + A^{--}(D^{++})^* - (A^{--})^* D^{++} \\ &+ A^{--}(C^{-+})^* - (A^{--})^* C^{-+} + B^{+-}(D^{++})^* - (B^{+-})^* D^{++}\} \\ &- (1-v) K_c k_s \omega \cos^2\theta_s \sin\theta_s\{|A^{--}|^2 + |B^{+-}|^2 - |C^{-+}|^2 - |D^{++}|^2 \\ &- A^{--}(B^{+-})^* - (A^{--})^* B^{+-} - B^{+-}(C^{-+})^* + (B^{+-})^* C^{-+} \\ &+ C^{-+}(D^{++})^* + (C^{-+})^* D^{++} - A^{--}(D^{++})^* + (A^{--})^* D^{++} \\ &- A^{--}(C^{-+})^* + (A^{--})^* C^{-+} - B^{+-}(D^{++})^* + (B^{+-})^* D^{++}\}], \end{aligned} \tag{36}$$

$$\begin{aligned}\langle e_s\rangle = &\tfrac{1}{4}\,\mathrm{Re}[G_c h |k_s|^2(\sin^4\theta_s - 2\sin^2\theta_s\cos^2\theta_s + \cos^4\theta_s)\{|A^{--}|^2 + |B^{+-}|^2 + |C^{-+}|^2 + |D^{++}|^2 \\ &+ A^{--}(B^{+-})^* + (A^{--})^* B^{+-} + B^{+-}(C^{-+})^* + (B^{+-})^* C^{-+} \\ &+ C^{-+}(D^{++})^* + (C^{-+})^* D^{++} + A^{--}(D^{++})^* + (A^{--})^* D^{++} \\ &+ A^{--}(C^{-+})^* + (A^{--})^* C^{-+} + B^{+-}(D^{++})^* + (B^{+-})^* D^{++}\} \\ &+ 2(1-v) K_c |k_s|^2 \cos^2\theta_s \sin^2\theta_s\{|A^{--}|^2 + |B^{+-}|^2 + |C^{-+}|^2 + |D^{++}|^2 \\ &- A^{--}(B^{+-})^* - (A^{--})^* B^{+-} + B^{+-}(C^{-+})^* + (B^{+-})^* C^{-+} \\ &- C^{-+}(D^{++})^* - (C^{-+})^* D^{++} + A^{--}(D^{++})^* + (A^{--})^* D^{++} \\ &- A^{--}(C^{-+})^* - (A^{--})^* C^{-+} - B^{+-}(D^{++})^* - (B^{+-})^* D^{++}\} \\ &+ \omega^2 \rho h \sin^2\theta_s\{|A^{--}|^2 + |B^{+-}|^2 + |C^{-+}|^2 + |D^{++}|^2 \\ &+ A^{--}(B^{+-})^* + (A^{--})^* B^{+-} - B^{+-}(C^{-+})^* - (B^{+-})^* C^{-+} \\ &+ C^{-+}(D^{++})^* + (C^{-+})^* D^{++} - A^{--}(D^{++})^* - (A^{--})^* D^{++} \\ &- A^{--}(C^{-+})^* - (A^{--})^* C^{-+} - B^{+-}(D^{++})^* - (B^{+-})^* D^{++}\} \\ &+ \omega^2 \rho h \cos^2\theta_s\{|A^{--}|^2 + |B^{+-}|^2 + |C^{-+}|^2 + |D^{++}|^2 \\ &- A^{--}(B^{+-})^* - (A^{--})^* B^{+-} - B^{+-}(C^{-+})^* - (B^{+-})^* C^{-+} \\ &- C^{-+}(D^{++})^* - (C^{-+})^* D^{++} - A^{--}(D^{++})^* - (A^{--})^* D^{++} \\ &+ A^{--}(C^{-+})^* + (A^{--})^* C^{-+} + B^{+-}(D^{++})^* + (B^{+-})^* D^{++}\}], \end{aligned} \tag{37}$$

where k_{sx} and k_{sy} are the x and y components of the complex in-plane wave number k_s respectively. For small damping, k_s, k_{sx} and k_{sy} are well approximated as

$$k_s = k_{s1}\left(1 - \mathrm{j}\frac{\eta_s}{2}\right), \quad k_{sx} = k_{sx1}\left(1 - \mathrm{j}\frac{\eta_s}{2}\right), \quad k_{sy} = k_{sy1}\left(1 - \mathrm{j}\frac{\eta_s}{2}\right), \tag{38}$$

where k_{s1}, k_{sx1} and k_{sy1} are the real parts of k_s, k_{sx} and k_{sy} respectively. In equation (35), the square terms, $|A^{--}|^2, \ldots, |D^{++}|^2$ are exponentially decayed in space due to structural damping and the other terms, $A^{--}(B^{+-})^*, \ldots, (B^{+-})^* D^{++}$ are spatially harmonic. At this stage, no obvious relations between intensity (equations (35) and (36)) and energy density (equation (37)) are found as in the previous case for longitudinal waves.

Assuming that the structural damping for the in-plane shear motion of the plate is sufficiently small, all of the second and higher order terms of η_s are neglected. Then the intensity and energy density are space-averaged over a half wavelength of the in-plane shear wave as follows [2]:

$$\langle \overline{e_s} \rangle = \frac{k_{sx1} k_{sy1}}{\pi^2} \int_0^{\pi/k_{sy1}} \int_0^{\pi/k_{sx1}} \langle e_s \rangle \, \mathrm{d}x \, \mathrm{d}y, \tag{39}$$

$$\langle \overline{\mathbf{q}_s} \rangle = \frac{k_{sx1} k_{sy1}}{\pi^2} \int_0^{\pi/k_{sy1}} \int_0^{\pi/k_{sx1}} \langle \mathbf{q}_s \rangle \, \mathrm{d}x \, \mathrm{d}y. \tag{40}$$

The space- and time-averaged intensity and energy density are obtained as

$$\langle \overline{q_{sx}} \rangle = \tfrac{1}{2} G h k_{sx1} \omega (|A|^2 e^{--} - |B|^2 e^{+-} + |C|^2 e^{-+} - |D|^2 e^{++}), \tag{41}$$

$$\langle \overline{q_{sy}} \rangle = \tfrac{1}{2} G h k_{sy1} \omega (|A|^2 e^{--} + |B|^2 e^{+-} - |C|^2 e^{-+} - |D|^2 e^{++}) \tag{42}$$

and

$$\langle \overline{e_s} \rangle = \tfrac{1}{2} G h k_{s1}^2 (|A|^2 e^{--} + |B|^2 e^{+-} + |C|^2 e^{-+} + |D|^2 e^{++}), \tag{43}$$

where for simplicity, $e^{\pm\pm} \equiv \exp(\pm \eta_s k_{sx1} x \pm \eta_s k_{sy1} y)$, and these three expressions are related in the following manner:

$$\langle \overline{\mathbf{q}_s} \rangle = -\frac{c_{gs}^2}{n_s \omega} \left(\frac{\partial}{\partial x} \mathbf{i} + \frac{\partial}{\partial y} \mathbf{j} \right) \langle \overline{e_s} \rangle. \tag{44}$$

Equation (44) is the expression for the energy transmission of in-plane shear waves in thin plates with damping and is analogous to Fourier's law of heat transfer.

The combination of equations (30), (31) and (44) yields an energy governing equation for the space- and time-averaged in-plane shear wave energy density in plates with the form

$$-\frac{c_{gs}^2}{\eta_s \omega} \left(\frac{\partial^2}{\partial x^2} + \frac{\partial^2}{\partial y^2} \right) \langle \overline{e_s} \rangle + \eta \omega \langle \overline{e_s} \rangle = 0, \tag{45}$$

where c_{gs} is the group velocity of in-plane shear waves in a plate expressed as follows and is equal to the phase velocity:

$$c_{gs} = \sqrt{\frac{G}{\rho}}. \tag{46}$$

Equation (45) is a differential equation for the in-plane shear waves assumed to be plane waves in a finite thin plate and the primary variable is the total in-plane shear wave energy density space-averaged over a half wavelength and time-averaged over one period.

6. POWER FLOW ANALYSIS OF FINITE COUPLED THIN PLATES

In this section, the time- and space-averaged energy density and intensity distributions for the flexural, longitudinal and in-plane shear waves of a coupled plate structure are predicted by using the energy governing equations of in-plane waves in finite thin plates, equations (30), (33), (44) and (45) and the equation of the flexural wave developed by Bouthier [2]. The coupled structure is composed of two thin plates connected at a certain angle and excited by a transverse harmonic point force. The power due to the exciting force is applied to plate I as shown in Figure 1, and zero energy outflow (intensity) boundary conditions for each wave component at the plate edges are used. To examine the partial transmission and reflection of the power at the plate joint, the wave transmission approach is applied [11]. Both plates I and II are $1\,\mathrm{m} \times 1\,\mathrm{m} \times 1\,\mathrm{mm}$ in dimensions. The Young's modulus of the plates is $E = 7{\cdot}1 \times 10^{10}\,\mathrm{N/m^2}$ and the mass density is $\rho = 2700\,\mathrm{kg/m^3}$.

The computations are performed by using the single Fourier series (the Lévy solution) approximation, which is commonly known to converge much faster than the double Fourier series (the Navier solution). Since the energy outflows at all edges perpendicular to the y-axis as seen in Figure 1 are zero, the energy density of each wave component can be expressed with the single cosine series of y as follows:

$$\langle \overline{e_\alpha} \rangle_i = \sum_{n=0}^{\infty} E_{\alpha in}(x) \cos\left(\frac{n\pi}{L_y} y\right). \tag{47}$$

Here, the subscript α indicates a longitudinal wave (l), an in-plane shear wave (s) or a flexural wave (f). The subscript i indicates the region ①, ② or ③, demarcated by the position of the input power and the joint of the two plates as illustrated in Figure 1(a) and 1(b). L_y is the length in the y direction of each plate. Substituting equation (47) into the energy governing equation of each wave component, the series coefficient of the energy density, $E_{\alpha in}(x)$, is expressed as

$$E_{\alpha in} = A_{\alpha in} \exp(-\lambda_{\alpha in} x) + B_{\alpha in} \exp(\lambda_{\alpha in} x), \tag{48}$$

where $\lambda_{\alpha in}^2 = (n\pi/L_y)^2 + (\eta_\alpha \omega / c_{g\alpha i})^2$, and the intensity of each wave type, $\langle \overline{\mathbf{q}_\alpha} \rangle_i$, is obtained from the following relation:

$$\langle \overline{\mathbf{q}_\alpha} \rangle_i = -\frac{c_{g\alpha i}^2}{\eta_\alpha \omega} \left(\frac{\partial}{\partial x}\mathbf{i} + \frac{\partial}{\partial y}\mathbf{j}\right) \langle \overline{e_\alpha} \rangle_i. \tag{49}$$

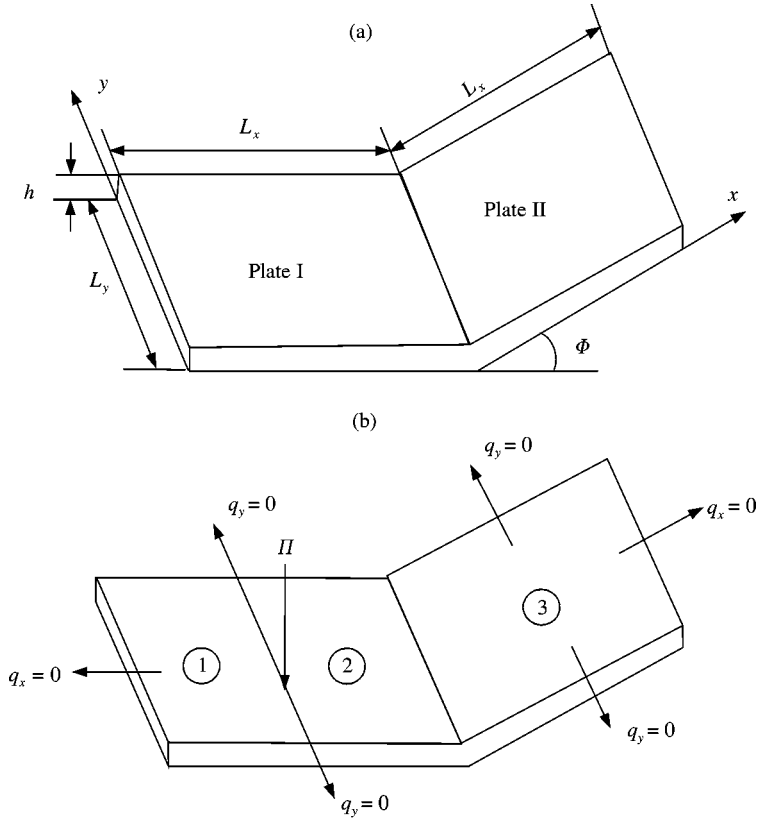

Figure 1. Two-plate structure coupled with a certain angle Φ and zero energy outflow boundary conditions; (a) dimensions of the structure, (b) zero energy flow boundary conditions.

The input power due to a point exciting force can also be expressed as

$$\Pi\delta(x - x_0)\delta(y - y_0) = \sum_{n=0}^{\infty} \Pi_n(x) \cos\left(\frac{n\pi}{L_y} y\right), \tag{50}$$

where Π is the magnitude of the input power and δ represents the Dirac delta function. x_0 and y_0 are the x and y positions of the exciting force. The series coefficient of the input power, $\Pi_n(x)$, can be obtained from the Fourier integral as follows:

$$\Pi_n(x) = \begin{cases} \dfrac{\Pi}{L_y}\delta(x - x_0) & (n = 0), \\ \dfrac{2\Pi}{L_y}\cos\left(\dfrac{n\pi}{L_y} y_0\right)\delta(x - x_0) & (n \neq 0). \end{cases} \tag{51}$$

To determine the unknowns $A_{\alpha in}$ and $B_{\alpha in}$ in equation (48), the energy and intensity boundary conditions are required. Since the energy outflows are zero at the edges perpendicular to the x-axis, we write

$$\langle \overline{q_{\alpha x}} \rangle_1 = 0, \quad \langle \overline{q_{\alpha x}} \rangle_3 = 0. \tag{52}$$

From the equilibriums of energy flow and the continuity of energy between regions ① and ②, the following relations are satisfied:

$$\langle \overline{q_{fx}} \rangle_2 - \langle \overline{q_{fx}} \rangle_1 = \Pi \delta(y - y_0), \tag{53}$$

$$\langle \overline{q_{lx}} \rangle_2 - \langle \overline{q_{lx}} \rangle_1 = 0, \quad \langle \overline{q_{sx}} \rangle_2 - \langle \overline{q_{sx}} \rangle_1 = 0, \tag{54}$$

$$\langle \overline{e_\alpha} \rangle_1 = \langle \overline{e_\alpha} \rangle_2. \tag{55}$$

At the joint of plates I and II, the incident waves are converted to other types of waves, and the power transmission and reflection of the incident wave must be examined. From the wave transmission approach, the power flows away from the joint in this plate are expressed as follows [11]:

$$\begin{aligned} \langle \overline{q_{fx}} \rangle_2^- = {} & \gamma_{ff22} \langle \overline{q_{fx}} \rangle_2^+ + \gamma_{lf22} \langle \overline{q_{lx}} \rangle_2^+ + \gamma_{sf22} \langle \overline{q_{sx}} \rangle_2^+ \\ & + \tau_{ff32} \langle \overline{q_{fx}} \rangle_3^- + \tau_{lf32} \langle \overline{q_{lx}} \rangle_3^- + \tau_{sf32} \langle \overline{q_{sx}} \rangle_3^-, \end{aligned} \tag{56}$$

$$\begin{aligned} \langle \overline{q_{lx}} \rangle_2^- = {} & \gamma_{fl22} \langle \overline{q_{fx}} \rangle_2^+ + \gamma_{ll22} \langle \overline{q_{lx}} \rangle_2^+ + \gamma_{sl22} \langle \overline{q_{sx}} \rangle_2^+ \\ & + \tau_{fl32} \langle \overline{q_{fx}} \rangle_3^- + \tau_{ll32} \langle \overline{q_{lx}} \rangle_3^- + \tau_{sl32} \langle \overline{q_{sx}} \rangle_3^-, \end{aligned} \tag{57}$$

$$\begin{aligned} \langle \overline{q_{sx}} \rangle_2^- = {} & \gamma_{fs22} \langle \overline{q_{fx}} \rangle_2^+ + \gamma_{ls22} \langle \overline{q_{lx}} \rangle_2^+ + \gamma_{ss22} \langle \overline{q_{sx}} \rangle_2^+ \\ & + \tau_{fs32} \langle \overline{q_{fx}} \rangle_3^- + \tau_{ls32} \langle \overline{q_{lx}} \rangle_3^- + \tau_{ss32} \langle \overline{q_{sx}} \rangle_3^-, \end{aligned} \tag{58}$$

$$\begin{aligned} \langle \overline{q_{fx}} \rangle_3^+ = {} & \tau_{ff23} \langle \overline{q_{fx}} \rangle_2^+ + \tau_{lf23} \langle \overline{q_{lx}} \rangle_2^+ + \tau_{sf23} \langle \overline{q_{sx}} \rangle_2^+ \\ & + \gamma_{ff33} \langle \overline{q_{fx}} \rangle_3^- + \gamma_{lf33} \langle \overline{q_{lx}} \rangle_3^- + \gamma_{sf33} \langle \overline{q_{sx}} \rangle_3^-, \end{aligned} \tag{59}$$

$$\begin{aligned} \langle \overline{q_{lx}} \rangle_3^+ = {} & \tau_{fl23} \langle \overline{q_{fx}} \rangle_2^+ + \tau_{ll23} \langle \overline{q_{lx}} \rangle_2^+ + \tau_{sl23} \langle \overline{q_{sx}} \rangle_2^+ \\ & + \gamma_{fl33} \langle \overline{q_{fx}} \rangle_3^- + \gamma_{ll33} \langle \overline{q_{lx}} \rangle_3^- + \gamma_{sl33} \langle \overline{q_{sx}} \rangle_3^-, \end{aligned} \tag{60}$$

$$\begin{aligned} \langle \overline{q_{sx}} \rangle_3^+ = {} & \tau_{fs23} \langle \overline{q_{fx}} \rangle_2^+ + \tau_{ls23} \langle \overline{q_{lx}} \rangle_2^+ + \tau_{ss23} \langle \overline{q_{sx}} \rangle_2^+ \\ & + \gamma_{fs33} \langle \overline{q_{fx}} \rangle_3^- + \gamma_{ls33} \langle \overline{q_{lx}} \rangle_3^- + \gamma_{ss33} \langle \overline{q_{sx}} \rangle_3^-. \end{aligned} \tag{61}$$

Here, the superscripts $(+)$ and $(-)$ represent wave propagation in the $+x$ and $-x$ directions respectively. $\tau_{\alpha\beta ij}$ is the β wave-type power transmission coefficient in region j due to the incident α wave type in region $i (i, j = 2, 3; \alpha, \beta = l, s, f)$, and $\gamma_{\alpha\beta ii}$ is the β wave-type power reflection coefficient in region i due to the incident α wave type in region i. Since the coefficients vary with the incidence angles, the mean coefficient values for the incidence angles were selected for the analysis by the assumption that the wave fields in the structure are well diffused. From the boundary conditions, the unknowns in each mode of the series are determined, and the energy and intensity for all wave types are finally obtained. To assure the convergence of the series, the lowest 100 modes are calculated and summed. The input power is located at $x_0 = 0{\cdot}5$ m and $y_0 = 0{\cdot}3$ m in plate I and its magnitude is 101·7 dB

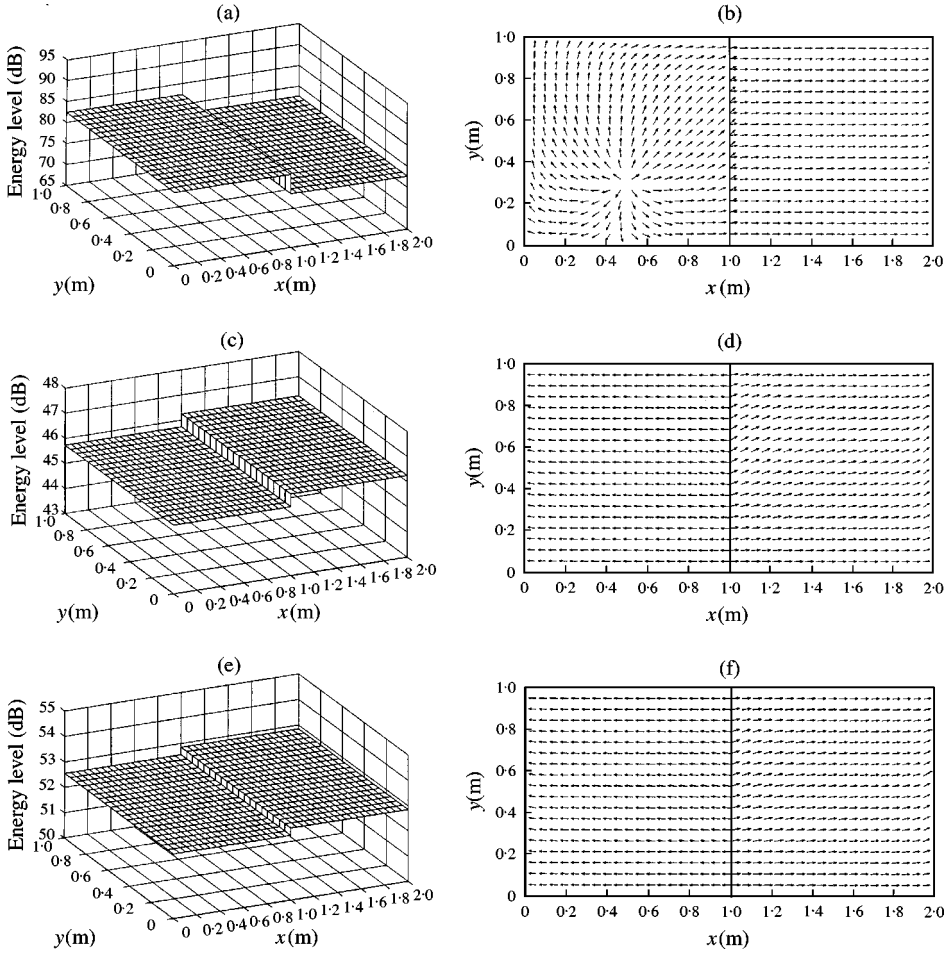

Figure 2. Energy and intensity distributions of two-plate structure coupled with $\Phi = 90^\circ$ when $f = 1$ kHz, $\eta = 0{\cdot}01$, $x_0 = 0{\cdot}5$ m and $y_0 = 0{\cdot}3$ m. The reference energy is 1×10^{-12} J/m^2 and the reference intensity is 1×10^{-12} W/m^2; (a) flexural wave energy, (b) flexural wave intensity, (c) longitudinal wave energy, (d) longitudinal wave intensity, (e) in-plane shear wave energy, (f) in-plane shear wave intensity.

re 1×10^{-12} W/m^2. The joint angle is $\Phi = 90^\circ$. The damping loss factors of three wave types are assumed to have the same value η.

In the first example, the frequency is $f = 1$ kHz and the damping loss factor is $\eta = 0{\cdot}01$. The flexural wave energy is discontinuous at the plate joint showing the lower level in plate II as seen in Figure 2(a), and the energy levels of longitudinal and in-plane waves are higher in plate II than in plate I as shown in Figure 2(c) and 2(e), as expected. The energy levels of all wave types are nearly constant in each plate. From the intensity distributions of Figure 2(b), 2(d) and 2(f), the power flow pattern of each wave is visualized.

In the second example, the damping is changed to $\eta = 0{\cdot}1$. The distributions of energy and intensity of three wave types are shown in Figure 3. The average energy level of flexural wave of this case is reduced by 10·1 dB compared with that of the first example and the average energy levels of longitudinal and in-plane waves are reduced by 17·5 and 17·8 dB respectively. The energy level of flexural wave is dissipated more rapidly than those of

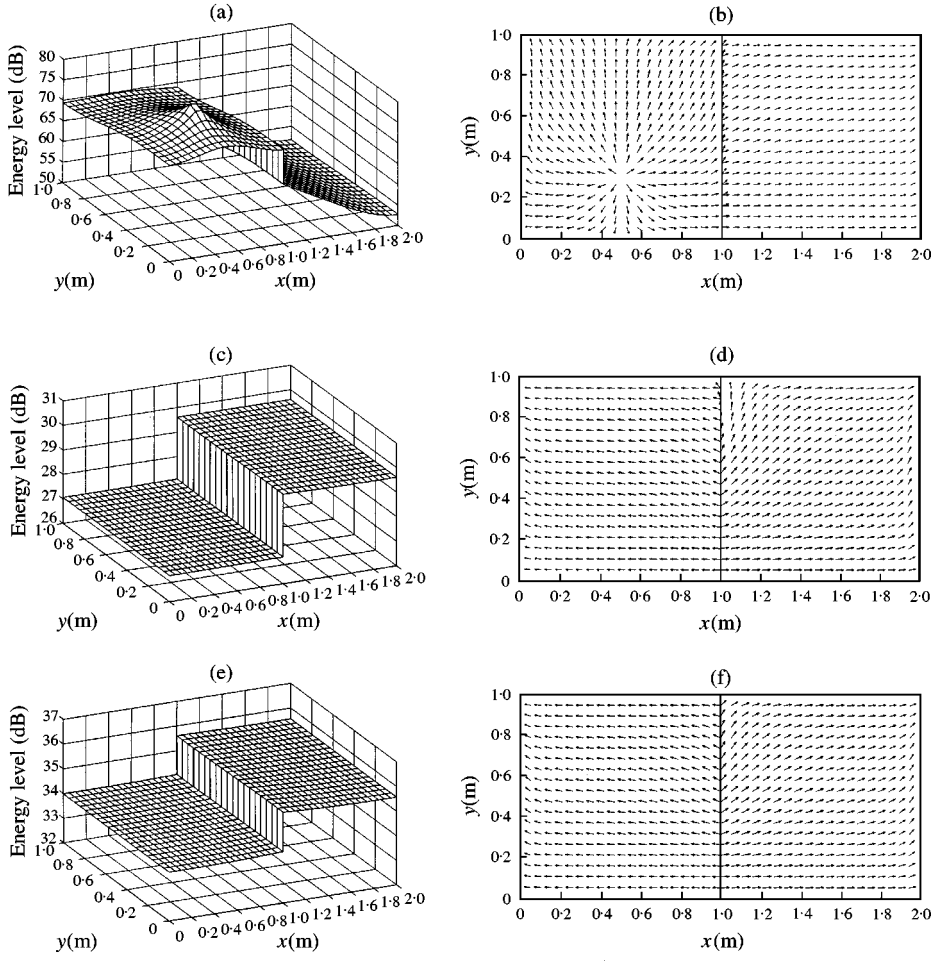

Figure 3. Energy and intensity distributions of two-plate structure coupled with $\Phi = 90^\circ$ when $f = 1$ kHz, $\eta = 0{\cdot}1$, $x_0 = 0{\cdot}5$ m and $y_0 = 0{\cdot}3$ m. The reference energy is 1×10^{-12} J/m^2 and the reference intensity is 1×10^{-12} W/m^2; (a) flexural wave energy, (b) flexural wave intensity, (c) longitudinal wave energy, (d) longitudinal wave intensity, (e) in-plane shear wave energy, (f) in-plane shear wave intensity.

in-plane waves which are still nearly constant in each plate because the group velocities of longitudinal and in-plane waves are much larger than that of flexural wave. It is shown that the energy difference of each wave between plates I and II at the joint is increased as the damping is increased. The corresponding intensity distributions are illustrated in Figure 3(b), 3(d) and 3(f).

In the next example, the frequency and the damping loss factor are $f = 10$ kHz and $\eta = 0{\cdot}01$ respectively. Comparing Figure 2 with Figure 4, the global variation of the energy increases and the average energy level is reduced as the frequency is increased. The energy transmission paths are not changed significantly. If the damping is increased to $\eta = 0{\cdot}1$ with the same frequency, the energies decrease more rapidly, as shown in Figure 5. It can be found that the in-plane wave energies have the maximum values at a place in the joint near the location of the input power. At the right end of plate II, the in-plane wave energies are higher than the flexural wave energy. From these results, it is verified that the in-plane

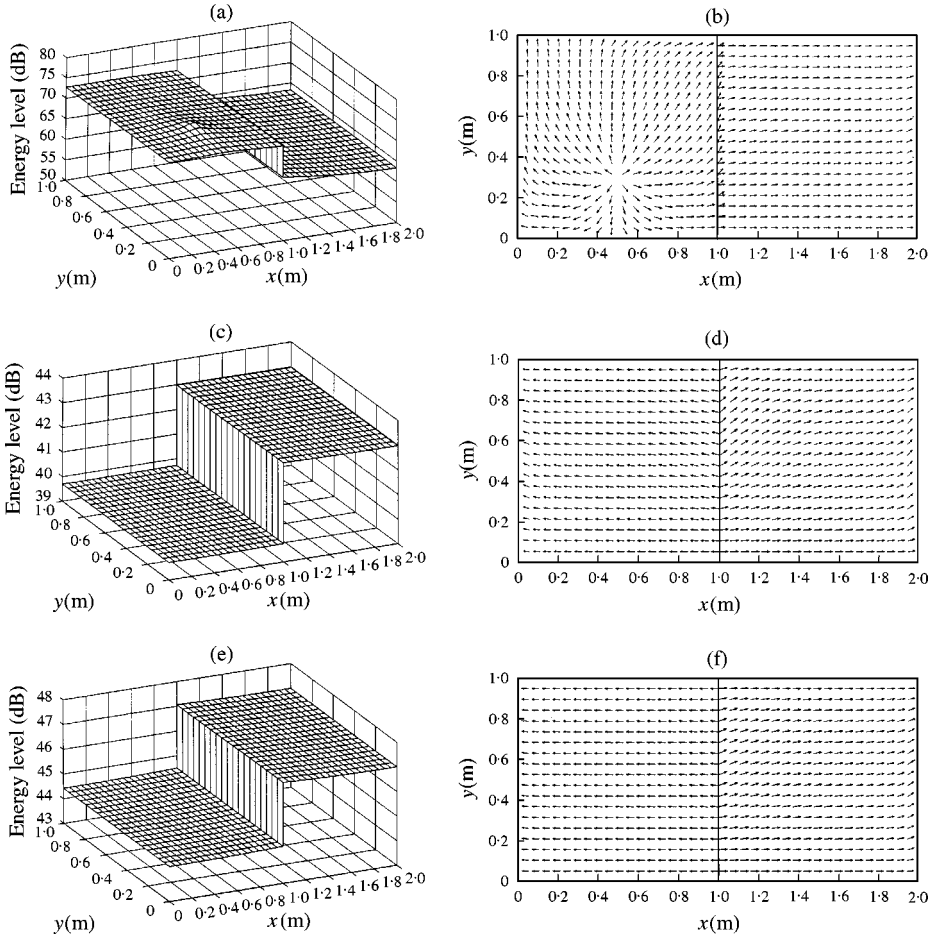

Figure 4. Energy and intensity distributions of two-plate structure coupled with $\Phi = 90^\circ$ when $f = 10\,\text{kHz}$, $\eta = 0{\cdot}01$, $x_0 = 0{\cdot}5\,\text{m}$ and $y_0 = 0{\cdot}3\,\text{m}$. The reference energy is $1 \times 10^{-12}\,\text{J/m}^2$ and the reference intensity is $1 \times 10^{-12}\,\text{W/m}^2$; (a) flexural wave energy, (b) flexural wave intensity, (c) longitudinal wave energy, (d) longitudinal wave intensity, (e) in-plane shear wave energy, (f) in-plane shear wave intensity.

waves are important in transmitting the vibration energy of a coupled plate structure with large damping at a high-frequency range. The corresponding intensity distributions are shown in Figure 5(b), 5(d) and 5(f).

In addition to the previous figures, Figure 6 shows the energy level of each wave type averaged through plate II as a dependent variable of the joint angle Φ varying from 0 to 90°. When the joint angle is 0° (a single-plate case), the average flexural wave energy level of plate II has maximum value, but in-plane wave energy levels are 0 dB, as shown in Figure 6. However, if the joint angle is slightly increased, in-plane wave energies increase very fast, but the flexural wave energy decreases a little. In the case that the frequency is $f = 1\,\text{kHz}$ and the damping is $\eta = 0{\cdot}01$, the energy level of every wave type has nearly constant values in the range where Φ is above about 20°, as shown in Figure 6(a). If the frequency is increased to $f = 10\,\text{kHz}$ on the same damping condition, the energy levels are nearly constant in the range above about 30°, as shown in Figure 6(c). When the damping is changed to $\eta = 0{\cdot}1$, the energy levels are shown in Figure 6(b) and 6(d).

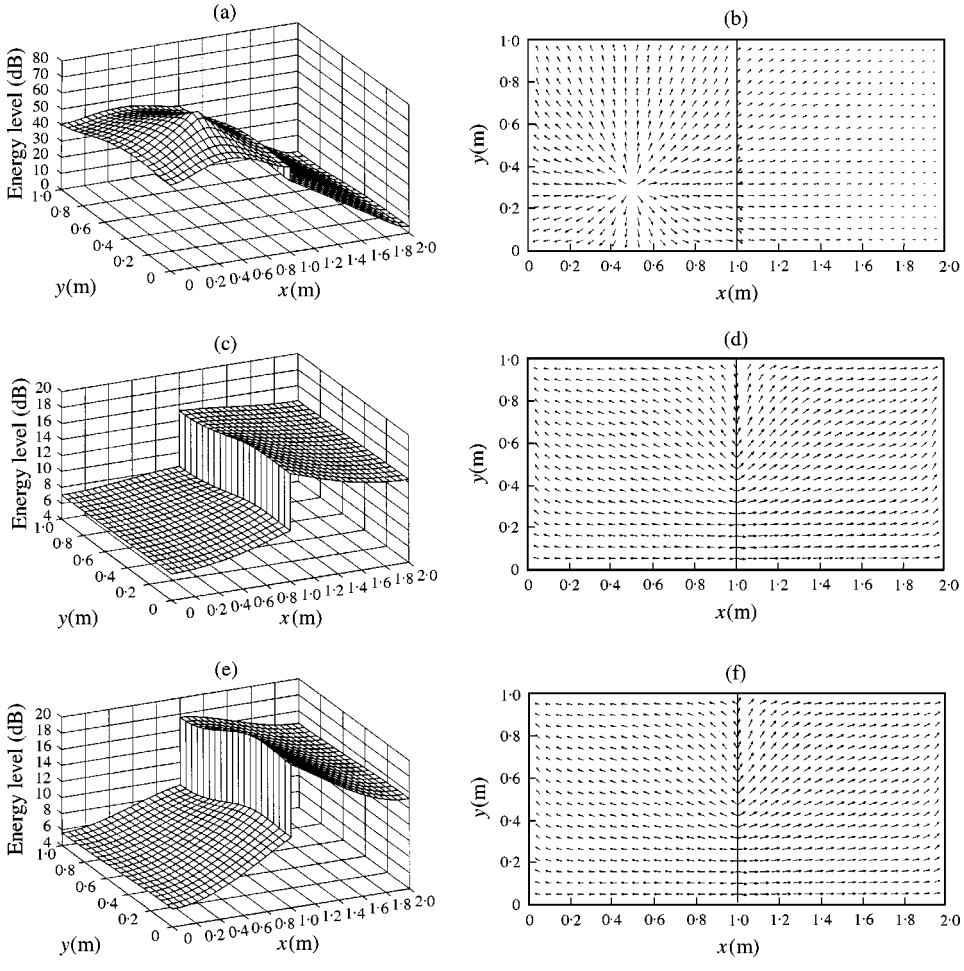

Figure 5. Energy and intensity distributions of two-plate structure coupled with $\Phi = 90^\circ$ when $f = 10\,\text{kHz}$, $\eta = 0{\cdot}1$, $x_0 = 0{\cdot}5\,\text{m}$ and $y_0 = 0{\cdot}3\,\text{m}$. The reference energy is $1 \times 10^{-12}\,\text{J/m}^2$ and the reference intensity is $1 \times 10^{-12}\,\text{W/m}^2$; (a) flexural wave energy, (b) flexural wave intensity, (c) longitudinal wave energy, (d) longitudinal wave intensity, (e) in-plane shear wave energy, (f) in-plane shear wave intensity.

7. CONCLUSIONS

Power flow models of finite thin plates have been developed for longitudinal and in-plane shear waves with the assumption that all of the waves are plane waves. The derived energy equations are applied to predict the energy and intensity distributions of a two-plate structure coupled at a certain angle. For finite coupled plates, it has been found that the in-plane wave energy levels are higher than those of the flexural waves at relatively high-frequency ranges and high damping when the transverse exciting force is applied to the structure. Moreover, the energy transmission paths are understood.

The derived power flow models can be used to predict the time- and space-averaged energy and intensity distributions of plate structures undergoing in-plane vibration in the middle–high-frequency ranges.

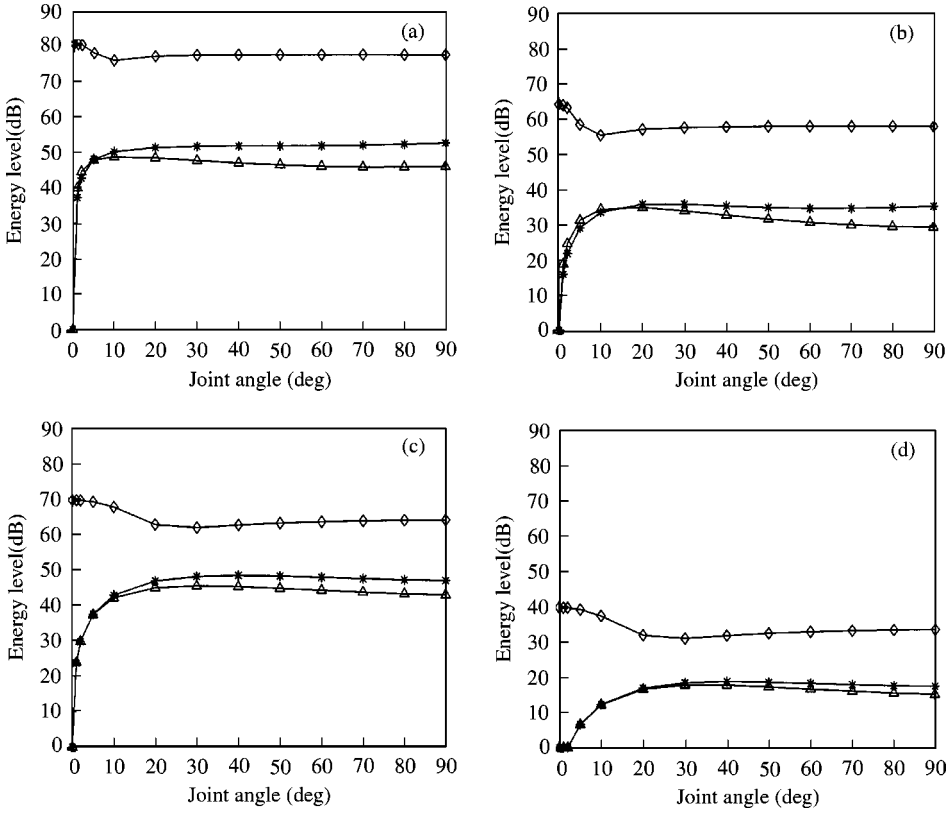

Figure 6. Average energy levels of plate II for various joint angles; (a) $f = 1$ kHz and $\eta = 0{\cdot}01$, (b) $f = 1$ kHz and $\eta = 0{\cdot}1$, (c) $f = 10$ kHz and $\eta = 0{\cdot}01$, (d) $f = 10$ kHz and $\eta = 0{\cdot}1$: -◇-, flexural wave energy; -△-, longitudinal wave energy; -*-, in-plane shear wave energy.

ACKNOWLEDGMENTS

The authors thank the Agency for Defense Development, which supported the research in this paper.

REFERENCES

1. O. M. BOUTHIER and R. J. BERNHARD 1995 *Journal of Sound and Vibration* **182**, 129–147. Simple models of the energy flow in vibrating membranes.
2. O. M. BOUTHIER and R. J. BERNHARD 1995 *Journal of Sound and Vibration* **182**, 149–164. Simple models of the energetics of transversely vibrating plates.
3. R. H. LYON 1986 *Journal of Noise Control Engineering* **26**, 22–27. In-plane contribution to structural noise transmission.
4. A. N. BERCIN 1996 *Journal of Sound and Vibration* **191**, 661–680. An assessment of the effects of in-plane vibrations on the energy flow between coupled plates.
5. J. D. ACHENBACH 1973 *Wave Propagation in Elastic Solids*. New York: Wiley Inc.
6. N. H. FALAG and J. PAN 1998 *Journal of the Acoustical Society of America* **103**, 408–413. Free and forced in-plane vibration of rectangular plates.

7. J. MIKLOWITZ 1978 *The Theory of Elastic Waves and Waveguides*. Amsterdam: North-Holland.
8. M. N. ICHCHOU and L. JEZEQUEL 1996 *Journal of Sound and Vibration* **195**, 679–685. Comments on simple models of the energy flow in vibrating membranes and on simple models of the energetics of transversely vibrating plates.
9. M. N. ICHCHOU, A. LE BOT and L. JEZEQUEL 1997 *Journal of Sound and Vibration* **201**, 535–554. Energy models of one-dimensional multi-propagative systems.
10. L. CREMER, M. HECKL and E. E. UNGAR 1988 *Structure-Borne Sound*. Berlin: Springer-Verlag.
11. P. E. CHO 1993 *Ph.D. Dissertation, Purdue University*. Energy Flow Analysis of Coupled Structures.